

Short Communication

Effect of Zinc Phosphating Pretreatment on NiP Electroless coating on AZ31B Magnesium Alloy Surface

Zhang Qingyu

College of Automotive Engineering, Henan Industry and Trade Vocational College, Zhengzhou, Henan, 451191, China

E-mail: zqy_college@sina.cn

Received: 14 February 2022 / *Accepted:* 3 April 2022 / *Published:* 7 May 2022

AZ31B is a kind of deformed magnesium alloys with good mechanical property, which is mainly used in the field of aerospace, new energy automobile, electronic products and so on. The ZnP is firstly deposited on the surface of AZ31B used for new energy automobile by phosphating pretreatment. And then, the electroless NiP coating is obtained on the surface of ZnP on AZ31B magnesium alloy. In order to further improve the hardness and corrosion resistance, the electroless NiP coating prepared on the surface of magnesium alloy is passivated finally. It is found out that the surface morphology of ZnP shows many micro cracks, which could disperse and decrease corrosion current. The micro cracks and zinc elements provide favorable nucleation conditions for the electroless NiP coating with better hardness and great corrosion resistance performance. Furthermore, the electroless NiP coating after passivation treatment has the largest hardness and the smallest corrosion current density, which are 417.51 HV_{0.1} and 12.58 $\mu\text{A}/\text{cm}^2$ respectively.

Keywords: AZ31B magnesium alloy; new energy automobile; phosphating; electroless NiP coating; passivation;

1. INTRODUCTION

Magnesium alloys possess many excellent properties, such as better ductility, lower density, excellent conductivity which are widely used in aerospace, automobile manufacturing, electronic products and other fields. Especially in the field of new energy automobile industry, magnesium alloys are considered as a kind of lightweight materials which can greatly reduce the mass of automobiles [1-3]. According to many reports, reducing the mass of a car by half will also reduce energy consumption by nearly half. Therefore, the use of magnesium alloy as lightweight materials in new energy automobiles can greatly save the energy consumption [4-7]. AZ31B magnesium alloy is a deformed magnesium alloy with good mechanical properties [8-10]. It is mainly used in the frame, skeleton, bottom plate and battery cover for new energy automobiles.

However, the chemical performance of AZ31B magnesium alloy is very active due to negative electrode potential, which is easy to be damaged by electrochemical corrosion. The poor corrosion resistance of AZ31B magnesium alloy seriously hinders its widespread application. At present, there are many methods to improve the corrosion resistance of magnesium alloys. The commonly used surface treatment technology mainly includes electroless plating, electroplating, phosphating and anodic oxidation [11-17]. Among them, phosphating and electroless plating possess the advantages of simple process, high efficiency and low cost which are widely used. However, the coating formed on magnesium alloy surface by phosphating treatment is thin and soft, which can only be partially used in surface decoration. In this paper, ZnP was prepared by phosphating treatment on AZ31B magnesium alloy surface. Then, NiP alloy coating was deposited on the surface of ZnP by electroless deposition. Finally, the electroless NiP coating was passivated to greatly improve corrosion resistance and hardness, which has a certain innovation.

2. EXPERIMENTAL

2.1 Pretreatment of AZ31B magnesium alloy

AZ31B magnesium alloy was used as the substrate in the experiment. The specific information about chemical composition of AZ31B is listed in Table 1.

Table 1 Chemical composition of AZ31B magnesium alloy

Substrate	Mg%	Al%	Si%	Ca%	Zn%	Mn%	Fe%	Cu%	Ni%
AZ31B	>93	2.5- 3.5	0.08	0.04	0.6- 1.4	0.2- 1.0	0.003	0.01	0.001

The AZ31B magnesium alloy was cut into 3 cm×3 cm×0.1 cm size as the substrate. Grind the substrate with 300 #, 600 #, 1000 # and 1200 # abrasive paper respectively until the surface is flat and bright to obtain a clean magnesium alloy substrate. Magnesium alloy may have oil stains in the process of grinding, so ultrasonic cleaning in anhydrous ethanol solution is used to dissolve oil stains on the surface of magnesium alloy for 10 min. After that, the alkali solution (15 % NaOH, 50 °C) and acid solution (30% HNO₃, 30 °C) were used to clean the substrate respectively. Finally, the substrate was cleaned by pure water and dried by a blower.

2.2 Phosphating and electroless deposition technique

Since magnesium alloy is active and has no autocatalytic performance, it is difficult to electroless NiP coating on magnesium alloy directly. Therefore, phosphating treatment for magnesium alloys is necessary before electroless deposition. The chemical composition of phosphating solution includes 10

g/L Na_2HPO_4 , 6 g/L $\text{Zn}(\text{NO}_3)_2$, 3 g/L NaNO_3 and 0.5 g/L NaF . The phosphating time is 25 min at the temperature of 50 °C. After phosphating, the surface of magnesium alloy contains metallic zinc labeled as ZnP/AZ31B in the paper, which is beneficial to electroless plating NiP alloy due to the autocatalytic effect of zinc.

An alkali electroless solution (5 g/L NiSO_4 , 10 g/L $\text{C}_6\text{H}_5\text{O}_7(\text{NH}_4)_3$, 3 g/L NaH_2PO_2 , 4 g/L H_3BO_3) was used to deposit NiP coating on the surface AZ31B magnesium alloy labeled as NiP/ZnP/AZ31B in the paper. The electroless deposition is 1 hour at the temperature of 90 °C in 200 mL solution with pH=10 (sodium hydroxide regulates the pH of the solution).

2.3 Passivation treatment

In order to further improve the corrosion resistance of NiP coating on magnesium alloy, passivation treatment is applied after electroless deposition to form passivated NiP/ZnP/AZ31B. The chemical solution is 25 g/L $\text{Cr}(\text{NO}_3)_3$, 12 g/L NaNO_3 , 10 g/L $\text{H}_2\text{C}_2\text{O}_4$, 10 g/L $\text{C}_3\text{H}_4\text{O}_4$. The passivation time is 3 min at pH=3 and 50 °C.

2.4 Experimental instruments and test methods

Scanning electron microscope (JCM7000) was used to observe the surface morphology of magnesium alloy and NiP coating. Digital Vickers hardness tester (HVT1000Z) was used to observe indentation and calculate Vickers hardness of samples. The surface roughness and element distribution were tested by the surface profile meter (MMD100A) and energy dispersive spectrometer (EDX300) respectively. The electrochemical workstation (CHI760e) was used to test the polarization curves of the sample to characterize the corrosion resistance. Meanwhile, the corrosion medium was 3.5% sodium chloride solution. The cathode was 1 cm × 1 cm NiP coating while the anode was 2 cm × 2 cm platinum electrode. The reference electrode was saturated calomel electrode, and the scanning rate was 1 mV/s.

3. RESULTS AND DISCUSSION

3.1 Surface morphology and roughness of coatings

Figure 1 shows the surface morphology of different coatings. The surface morphology of AZ31B magnesium alloy can be seen in Figure 1(a) which shows many pores and some scratches. Magnesium alloys is easily oxidized in the air to form a thin and loose oxide layer. The surface morphology of AZ31B magnesium after phosphating treatment is shown in Figure 1(b). A compact coating with many fine micro cracks can be formed on the surface of magnesium alloy after phosphating treatment. The cracks on the ZnP coating are circular and interlaced. Some researchers also report ZnP coating with cracks and other morphology, which may be related to the different composition of phosphating solutions [18-20]. Although the ZnP coating on magnesium alloy surface is thin, it has good adhesion. The obvious micro cracks on the surface of ZnP coating provide favorable nucleation conditions for the subsequent

electroless NiP deposition. The NiP particles will firmly adhere to the cracks. This can improve the adhesion between NiP coating and ZnP coating. The surface morphology of electroless NiP coatings can be seen in Figure 1(c) which shows rice shape morphology with relatively compact surface. In addition to rice shape morphology, electroless NiP coatings with nodular shape are also reported in some literatures [21-22]. According to Figure 1(d), after passivation treatment, the surface compactness of NiP coating is further improved and the porosity is greatly reduced, which is mainly attributed to the large amount of zinc hydroxide and chromium oxide filling the gap of NiP particles in the passivation process.

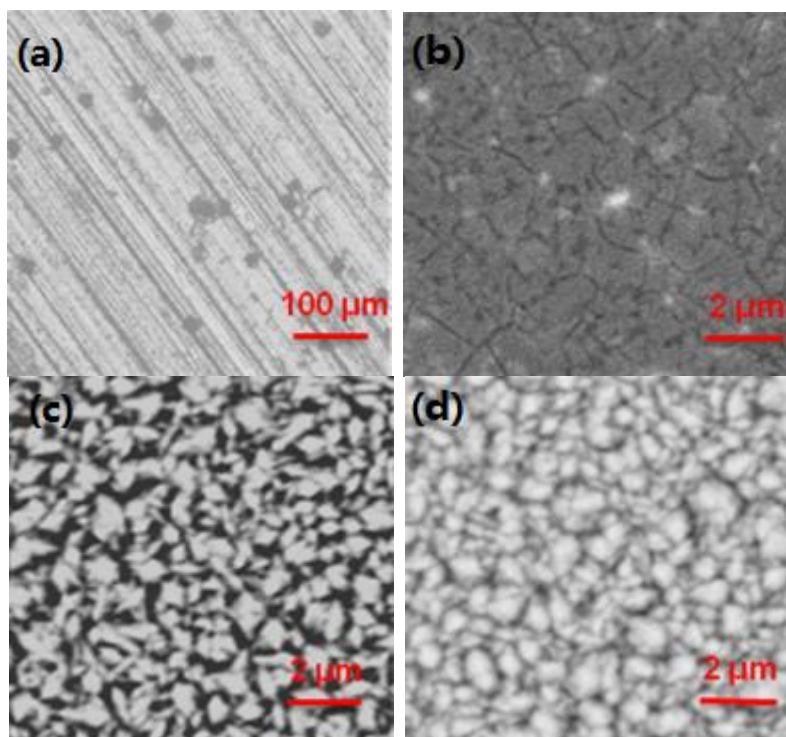


Figure 1. Surface morphology of different coatings; (a) AZ31B magnesium alloy; (b) ZnP/AZ31B; (c) NiP/ZnP/AZ31B; (d) Passivated NiP/ZnP/AZ31B;

Roughness of different coatings is tested by profile meter. In order to make the result more precise, roughness of three scanning lines with 500 μm length are averaged. The result is shown in Figure 2 and Table 2. Compared with other samples, the roughness of magnesium alloy is the largest, about 1.978 μm . The chemical property of magnesium alloy is too active, which can be oxidized into loose and rough oxide coating in the air resulting in rougher surface. After phosphating treatment, the roughness of magnesium alloy is reduced by half which is about 0.881 μm . There are many micro cracks on the surface of the ZnP coating, and NiP particles are adsorbed on the surface of the cracks to effectively reduce the roughness. After passivation treatment, a large amount of zinc hydroxide and chromium oxide fill the gap between NiP particles, which greatly improves the surface density resulting in minimum roughness equal to only 0.293 μm .

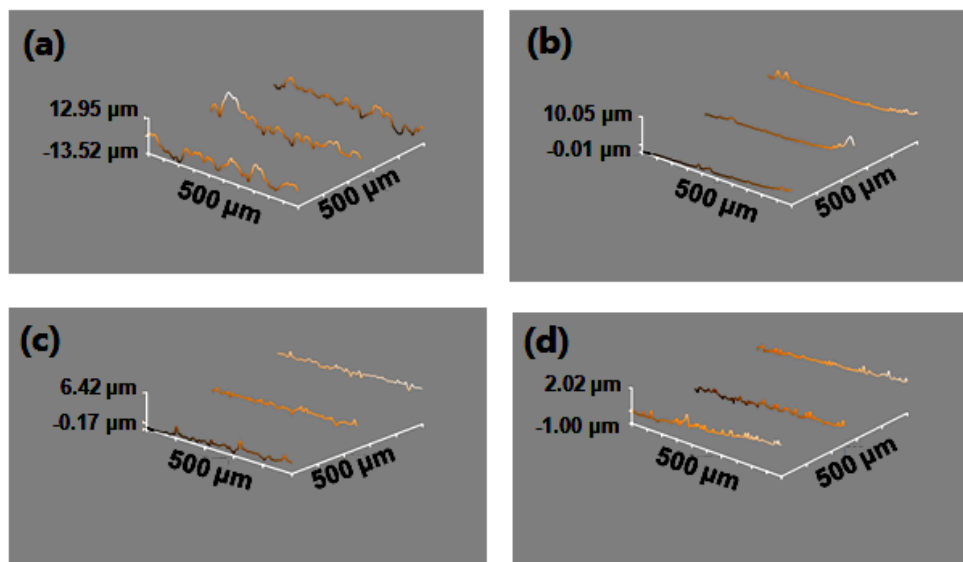


Figure 2. Surface roughness of different coatings; (a) AZ31B magnesium alloy; (b) ZnP/AZ31B; (c) NiP/ZnP/AZ31B; (d) Passivated NiP/ZnP/AZ31B; X scan size 500 μm; Y scan size 500 μm; Scan rate 5 μm/s;

Table 2 Roughness of different coatings

Specimen	Roughness of curve 1/ μm	Roughness of curve 2/ μm	Roughness of curve 3/ μm	Average roughness/ μm
a	2.102	2.203	1.629	1.978
b	0.893	0.823	0.928	0.881
c	0.492	0.502	0.513	0.502
d	0.302	0.293	0.283	0.293

3.2 Composition and hardness of coatings

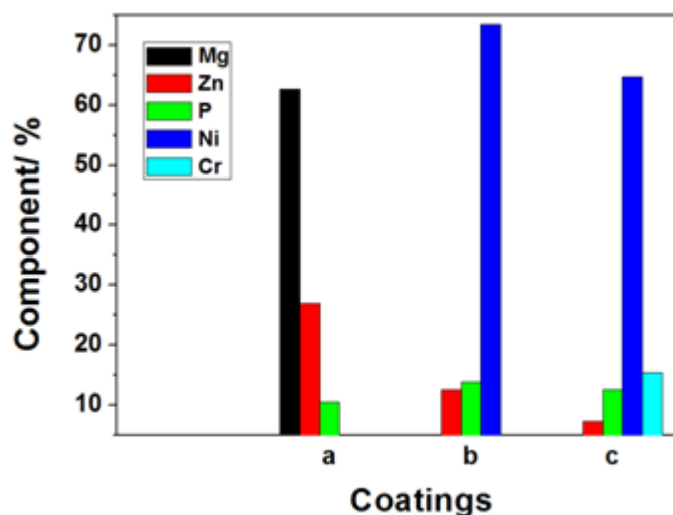


Figure 3. Elements distribution on the surface of coatings; (a) AZ31B magnesium alloy; (b) ZnP/AZ31B; (c) NiP/ZnP/AZ31B; (d) Passivated NiP/ZnP/AZ31B;

Table 3. Composition of different coatings

Specimen	Mg /%	Zn /%	P /%	Ni /%	Cr /%
a	62.6	26.9	10.5	-	-
b	-	12.6	13.9	73.5	-
c	-	7.3	12.6	64.7	15.4

The main elements distribution on the surface of ZnP/AZ31B is magnesium, zinc and phosphorus respectively. Magnesium alloy will be dissolved in acid phosphating solution, and the chemical reaction is as follows:



Only when the rate of ZnP coating formation is greater than the dissolution rate of magnesium alloy, the ZnP coating can be obtained on the surface of magnesium alloy [23-24]. Phosphorus and zinc come from Na₂HPO₄ and Zn(NO₃)₂ in the phosphating solution.

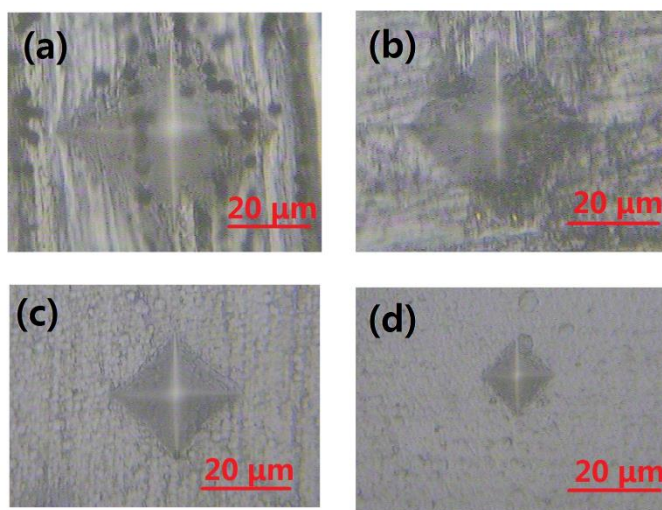
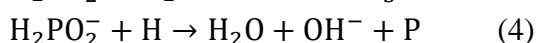
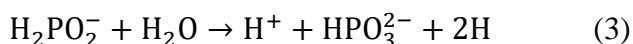


Figure 4. Surface morphology of indentation during Vickers hardness testing; (a) AZ31B magnesium alloy; (b) ZnP/AZ31B; (c) NiP/ZnP/AZ31B; (d) Passivated NiP/ZnP/AZ31B; The pressure force is 0.1 kg with 15 s hold time;

There are some micro cracks on the surface of ZnP coating, and the NiP particles can be deposited on the surface of these uneven cracks to form a continuous and compact NiP coating. The electroless NiP coating is composed of zinc, nickel and phosphorus. Since magnesium alloy has no autocatalytic activity, zinc on the surface is used as the nucleation area for electroless deposition of NiP. The deposition mechanism of electroless NiP coating is listed in equation (2)~(4).



The surface element distribution of NiP/ZnP/AZ31B after passivation treatment includes zinc, phosphorus, nickel and chromium which originates from zinc hydroxide and chromium oxide filling the gap of NiP particles in the passivation process.

The indentations of different specimens during Vickers hardness testing are characterized and hardness of each coating is calculated based on the area of indentation seen in Figure 4 and Figure 5. According to the results, the Vickers hardness of AZ31B magnesium alloy is approximate 74.66 HV_{0.1} due to loose and porous oxide coating in the surface. After the phosphating treatment, the hardness increases to about 121.19 HV_{0.1}. The hardness of electroless NiP coating is up to 295.92 HV_{0.1}, because the NiP particles firmly adhere to the cracks on the ZnP coating will improve the adhesion and hardness. It is found out that the passivated NiP/ZnP/AZ31B possesses the maximum hardness equal to 417.51 HV_{0.1}.

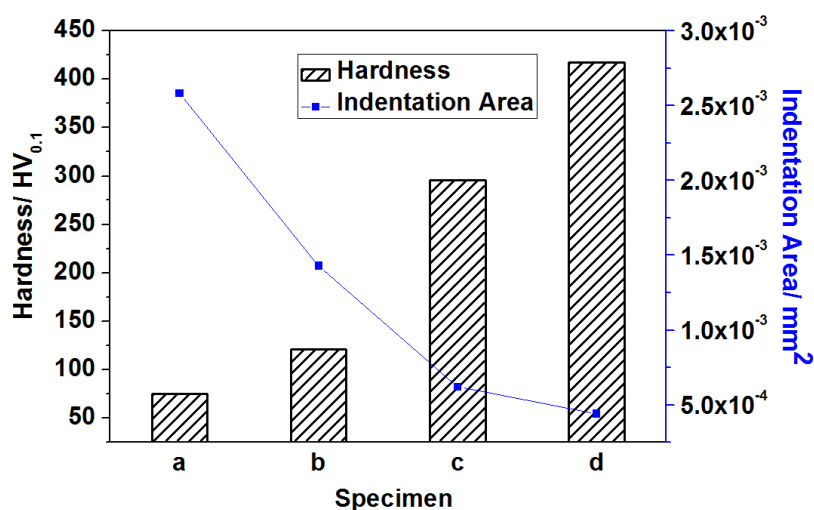


Figure 5. Vickers hardness of different coatings calculated based on the area of indentation; (a) AZ31B magnesium alloy; (b) ZnP/AZ31B; (c) NiP/ZnP/AZ31B; (d) Passivated NiP/ZnP/AZ31B; The pressure force is 0.1 kg with 15 s hold time;

3.3 Corrosion resistance of coatings

Polarization curves of different coatings in 3.5 % sodium chloride solution are shown in Figure 6. The self corrosion potential, corrosion current density and anodic Tafel slope are calculated and listed in Table 4. The self corrosion potential of AZ31B magnesium alloy substrate is the most negative, which is -1.28 V. Compared with the magnesium alloy substrate, after phosphating and electroless treatment, the self corrosion potential of magnesium alloy has different degrees of positive shift and the anodic Tafel slope increases gradually. The corrosion current density of AZ31B magnesium alloy is 154.88 $\mu\text{A}/\text{cm}^2$. However, the corrosion current density decreases to 47.86 $\mu\text{A}/\text{cm}^2$ and 12.58 $\mu\text{A}/\text{cm}^2$ respectively after the treatment of phosphating and electroless NiP. There are many micro cracks on the surface of ZnP coating, which can disperse and reduce the corrosion current during electrochemical corrosion. The autocatalytic action of zinc on the surface is beneficial to accelerate electroless deposition

of NiP, which improves the compactness and further reduces the corrosion current. The autocatalytic deposition mechanism of electroless NiP is investigated in some paper [25-26]. The passivated NiP/ZnP/AZ31B has the best corrosion resistance with the minimum corrosion current density due to large amounts of chromium oxide and hydroxide of zinc doped in the gaps of NiP particles.

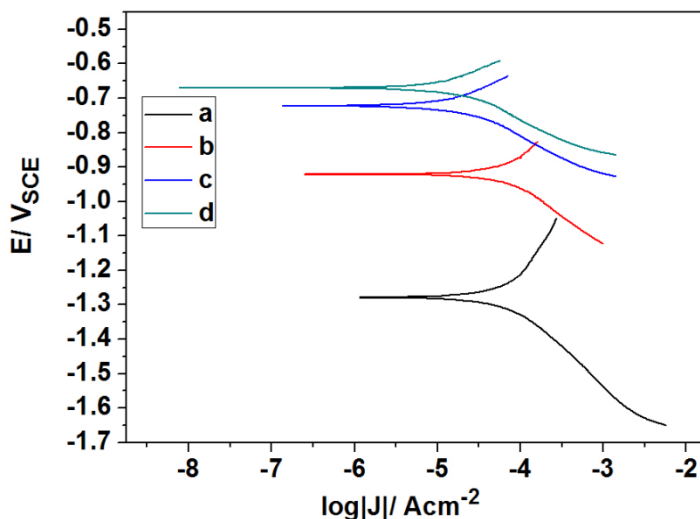


Figure 6. Polarization curves of coatings in 3.5% sodium chloride solution with 1 mV/s scanning rate; (a) AZ31B magnesium alloy; (b) ZnP/AZ31B; (c) NiP/ZnP/AZ31B; (d) Passivated NiP/ZnP/AZ31B;

Table 4. Parameters calculated from polarization curves

Specimen	E_{corr}/V	$J_{corr}/\mu A/cm^2$	Tafel slop B_a mV/dec
a	-1.281	154.88	102
b	-0.922	47.86	118
c	-0.723	12.58	143
d	-0.671	8.31	172

4. CONCLUSIONS

The NiP coating was prepared on the surface of AZ31B magnesium alloy after phosphating treatment. The surface morphology, composition, hardness, roughness and corrosion resistance of AZ31B magnesium, ZnP/AZ31B, NiP/ZnP/AZ31B and passivated NiP/ZnP/AZ31B were investigated. Many fine micro cracks can be formed on the surface of magnesium alloy after phosphating treatment, which provide favorable nucleation conditions for the electroless NiP deposition with relatively dense surface. The hardness and corrosion resistance of magnesium alloy both increase greatly after phosphating and electroless NiP. Moreover, after the passivation treatment, the NiP/ZnP/AZ31B

possesses the highest hardness and the minimum corrosion current density, which are 417.51 HV_{0.1} and 12.58 $\mu\text{A}/\text{cm}^2$ respectively.

ACKNOWLEDGEMENTS

This research is supported by science and technology project of Henan Province in the field of high and new technology (182102210097).

References

1. S. V. S. Prasad, S. B. Prasad, K. Verma, R. K. Mishra, V. Kumar and S. Singh, *J. Magnesium Alloys*, 10 (2022) 1.
2. D. Kumar, R. K. Phanden and L. Thakur, *Mater. Today: Proc.*, 38 (2021) 359.
3. X. Zhao, P. C. Gao, G. Chen, J. F. Wei, Z. Zhu, F. F. Yan, Z. M. Zhang and Q. Wang, *Mater. Sci. Eng. A*, 799 (2021) 140366.
4. J. D. Du, W. J. Han and Y. H. Peng, *J. Cleaner Prod.*, 18 (2010) 112.
5. M. Hakamada, T. Furuta, Y. Chino, Y. Q. Chen, H. Kusuda and M. Mabuchi, *Energy*, 32 (2007) 1352.
6. R. Kawalla, G. Lehmann, M. Ullmann and H. P. Vogt, *Arch. Civ. Mech. Eng.*, 8 (2008) 93.
7. K. Kawajiri, M. Kobayashi and K. Sakamoto, *J. Cleaner Prod.*, 253 (2020) 119805.
8. S. J. Chen, L. Wang, X. Q. Jiang, T. Yuan, W. Jiang and Y. Y. Liu, *J. Manuf. Processes*, 71 (2021) 317.
9. E. Garlea, M. Radovic and P. K. Liaw, *Mater. Sci. Eng. A*, 758 (2019) 86.
10. G. Chen, Y. J. Fu, Y. Cui, J. W. Gao, X. Guo, H. Gao, S. Z. Wu, J. Lu, Q. Lin and S. W. Shi, *Int. J. Fatigue*, 127 (2019) 461.
11. A. Anawati, E. Hidayati and H. Labibah, *Mater. Sci. Eng. B*, 272 (2021) 115354.
12. T. X. Wang, S. Q. Jia, Y. C. Xu, Y. Q. Dong, Y. T. Guo, Z. L. Huang, G. Y. Li and J. S. Lian, *Prog. Org. Coat.*, 163 (2022) 106653.
13. Q. Wu, B. X. Yu, P. Zhou, T. Zhang and F. H. Wang, *Mater. Chem. Phys.*, 273 (2021) 125121.
14. C. Yang, H. Cai, S. H. Cui, J. Huang, J. Y. Zhu, Z. C. Wu, Z. Y. Ma, R. K. Y. Fu, L. Y. Sheng, X. B. Tian, P. K. Chu and Z. Z. Wu, *Surf. Coat. Technol.*, 433 (2022) 128148.
15. R. Askarnia, S. R. Fardi, M. Sobhani, H. Staji and H. Aghamohammadi, *J. Alloys Compd.*, 892 (2022) 162106.
16. D. F. Carrillo, A. Bermudez, M. A. Gomez, A. A. Zuleta, J. G. Gastano and S. Mischler, *Surf. Interfaces*, 21 (2020) 100733.
17. S. Y. Jian, J. K. Chang, K. F. Lin, T. Y. Chen, J. H. Yuan and M. D. Ger, *Surf. Coat. Technol.*, 394 (2020) 125724.
18. X. J. Jia, J. F. Song, B. Q. Xiao, Q. Liu, H. Zhao, Z. Y. Yang, J. Liao, L. Y. Wu, B. Jiang, A. Atrens and F. S. Pan, *J. Mater. Res. Technol.*, 14 (2021) 1739.
19. H. L. Liu, Z. P. Tong, Y. Yang, W. F. Zhou, J. N. Chen, X. Y. Pan and X. D. Ren, *J. Alloys Compd.*, 865 (2021) 158701.
20. W. Zai, Y. C. Su, H. C. Man, J. S. Lian and G. Y. Li, *Appl. Surf. Sci.*, 492 (2019) 314.
21. X. S. Zhang, Q. Y. Wang, Y. R. Tang, H. C. Guo, Y. C. Xi, L. J. Dong and H. B. Zheng, *Int. J. Electrochem. Sci.*, 15 (2020) 11821.
22. H. Algul, M. Uysal and A. Alp, *Appl. Surf. Sci. Adv.*, 4 (2021) 100089.
23. C. Y. Zhang, S. J. Liao, B. X. Yu, X. P. Lu, X. B. Chen, T. Zhang and F. H. Wang, *Corros. Sci.*, 150 (2019) 279.
24. N. V. Phuong, K. H. Lee, D. Y. Chang and S. M. Moon, *Corros. Sci.*, 74 (2013) 314.
25. P. L. Cavallotti, L. Magagnin and C. Cavallotti, *Electrochim. Acta*, 114 (2013) 805.

26. C. P. Lin, M. Saito and T. Homma, *Electrochim. Acta*, 82 (2012) 75.

© 2022 The Authors. Published by ESG (www.electrochemsci.org). This article is an open access article distributed under the terms and conditions of the Creative Commons Attribution license (<http://creativecommons.org/licenses/by/4.0/>).